Spin-dependent exciton-exciton interaction potential in two- and three-dimensional semiconductors under excitation

Spin-dependent exciton–exciton interaction potential in two- and three-dimensional semiconductors under excitation

Nguyen Ba An†‖, Hoang Ngoc Cam‡ and Nguyen Trung Dan§

† International Centre for Theoretical Physics, Trieste, Italy
‡ Institute of Theoretical Physics, PO Box 429, Bo Ho, Hanoi 10000, Vietnam
§ Hue State University, 3 Le Loi, Hue, Vietnam

Abstract. Analytical expressions for the exciton–exciton interaction potentials have been approximately derived in both 2D and 3D materials exhibiting explicit dependences on exciton momentum difference, momentum transfer, electron–hole effective mass ratio and two-exciton state spin symmetry. Numerical calculations show that the character of the exciton–exciton interaction is determined by all of the above-mentioned dependences.

1. Introduction

Of particular importance is the exciton–exciton interaction, which has been studied in more or less detail within different approaches in both three- [1–20] and two-dimensional (3D and 2D) [20–27] excited materials. Disregarding spins of electrons and holes, the exciton–exciton interaction is mostly repulsive. Its Fourier transforms taken at zero momentum transfer $q = 0$ and at equal momenta of colliding excitons $p = p'$ take the values $13\pi I_{3D} r_{3D}^3 V_{3D}^{-1}/3$ [2–9] and $4\pi I_{2D} r_{2D}^2 V_{2D}^{-1}(1-315\pi^2/4096)$ [21, 26, 27] in the 'bulk' and 'planar' cases, respectively ($I_{3D(2D)}$, $r_{3D(2D)}$ and $V_{3D(2D)}$ are the 3D (2D) exciton binding energy, Bohr radius and sample volume (area)). For the practical purpose of quantitative comparison between theoretical calculations and experimental measurements, it is necessary to know the exciton–exciton interaction potential in the whole range of momentum transfer q and exciton momenta p, p' as well as of electron–hole effective mass ratio s. For example, to obtain the density-dependent exciton level shift and damping of a certain medium, one has to integrate expressions containing the exciton–exciton interaction potential over the whole range of q, p and p' with a given s (see, e.g., [20, 24, 28]). Since exact analytical evaluation of the exciton–exciton interaction potential is impossible, appropriate approximations must be invoked. In [20] an improved version of the approximation mentioned in [29] is proposed to derive explicit expressions for the exciton–exciton interaction potential that depend analytically on q, p, p' and s. Nevertheless, the spin of quasiparticles was not taken into account in [20] and, thus, collective phenomena such as the formation of biexcitons or electron–hole drop condensation, etc, could not be explained.

‖ Permanent address: Institute of Theoretical Physics, PO Box 429, Bo Ho, Hanoi 10000, Vietnam.

In this paper we deal with the analytical derivation of the explicit dependences of the exciton–exciton interaction potential not only on q, p, p' and s but also on the spin symmetry of the two excitons that interact. We shall show that the character of the exciton–exciton interaction should be determined by all of the above variables, i.e. by q, p, p', s and spin symmetry.

Throughout this paper the unit system with $\hbar = c = 1$ is used, where $\hbar$ and c are the Planck constant and the light velocity.

2. Spin-dependent interaction Hamiltonian in terms of exciton operators

Consider for simplicity a direct-gap, two-band semiconductor, which under band-to-band excitation comprises electrons and holes interacting between themselves via Coulomb force F_q. The original fermionic Hamiltonian of the semiconductor reads

$$
H^{\mathrm{eh}} = \sum_{kj_z^e} E_{e\Gamma_{j^e}j_z^e}(k)\, e^+_{k\Gamma_{j^e}j_z^e}\, e_{k\Gamma_{j^e}j_z^e} + \sum_{kj_z^h} E_{h\Gamma_{j^h}j_z^h}(k)\, h^+_{k\Gamma_{j^h}j_z^h}\, h_{k\Gamma_{j^h}j_z^h}
$$

$$
+ \tfrac{1}{2} \sum_{pp'q} F_q \Bigg(\sum_{j_z^e j_z'^e} e^+_{p+q,\Gamma_{j^e}j_z^e}\, e^+_{p'-q,\Gamma_{j^e}j_z'^e}\, e_{p'\Gamma_{j^e}j_z'^e}\, e_{p\Gamma_{j^e}j_z^e}
$$

$$
+ \sum_{j_z^h j_z'^h} h^+_{p+q,\Gamma_{j^h}j_z^h}\, h^+_{p'-q,\Gamma_{j^h}j_z'^h}\, h_{p'\Gamma_{j^h}j_z'^h}\, h_{p\Gamma_{j^h}j_z^h}
$$

$$
- 2 \sum_{j_z^e j_z^h} e^+_{p+q,\Gamma_{j^e}j_z^e}\, h^+_{p'-q,\Gamma_{j^h}j_z^h}\, h_{p'\Gamma_{j^h}j_z^h}\, e_{p\Gamma_{j^e}j_z^e} \Bigg). \tag{1}
$$

In (1), j^e (j^h) and j_z^e (j_z^h) label the electron (hole) total angular momentum and its projection on the z axis. Γ_{j^e} and Γ_{j^h} are the irreducible representations of the crystal symmetry group according to which the basic state vectors

$$
e^+_{k\Gamma_{j^e}j_z^e} |0\rangle = \psi_{e\Gamma_{j^e}j_z^e}\, e_k^+ |0\rangle \tag{2}
$$

and

$$
h^+_{k\Gamma_{j^h}j_z^h} |0\rangle = \psi_{h\Gamma_{j^h}j_z^h}\, h_k^+ |0\rangle \tag{3}
$$

are respectively transformed. In (2) and (3), $\psi_{e\Gamma_{j^e}j_z^e}$ ($\psi_{h\Gamma_{j^h}j_z^h}$) denote the j_z^e (j_z^h) component of the electron (hole) wavefunction in the conduction (valence) band at the centre of the Brillouin zone; and e_k^+ (h_k^+) creates an electron (a hole) with momentum k and energy $E_{e\Gamma_{j^e}j_z^e}(k)$ ($E_{h\Gamma_{j^h}j_z^h}(k)$). If the electron–hole pair is bound into the exciton in the state of relative motion characterized by the partners f_{nlm} of the irreducible representation D_l, then the basic state vectors of the exciton will be transformed according to the direct-product representation

$$
\Gamma_{j^e} \otimes \Gamma_{j^e} \otimes D_l = \sum_{j^a} \oplus\, \Gamma_{j^a}. \tag{4}
$$

The number of j^a will depend on the chosen scheme of the vectorial addition between the three angular momenta j^e, j^h and l. There may exist several addition schemes, which, however, are related to each other by unitary transformations [30]. Assume for definiteness that j^e first couples with j^h to form intermediate j^{eh}, which are then added to l. This assumption permits us to build by group-theoretical methods the creation

operator of the exciton with usual momentum k, total angular momentum j^a and its projection j_z^a in the form

$$a^+_{knlj^{eh}j^a j_z^a} = V^{-1/2} \sum_{pmj_z^e j_z^h} S^l_{mj_z^e j_z^h}(j^{eh}, j^a, j_z^a) f_{nlm}(p - \beta k)\, e^+_{k-p,\Gamma j^e j_z^e}\, h^+_{p\Gamma j^h j_z^h} \qquad (5)$$

where the presence of j^{eh} in (5) indicates the concrete vectorial addition scheme used, $\beta = (1 + s)^{-1}$ and

$$S^l_{mj_z^e j_z^h}(j^{eh}, j^a, j_z^a) = \sum_{j_z^{eh}} (j^e j_z^e j^h j_z^h | j^{eh} j_z^{eh})(j^{eh} j_z^{eh}\, lm | j^a j_z^a) \qquad (6)$$

with $(j^a j_z^a j^b j_z^b | jj_z)$ being the Clebsch–Gordan coefficients. Applying the well known properties of the Clebsch–Gordan coefficients helps us to verify that

$$\sum_{j^{eh}j^a j_z^a} S^l_{mj_z^e j_z^h}(j^{eh}, j^a, j_z^a) S^l_{m'j_z'^e j_z'^h}(j^{eh}, j^a, j_z^a) = \delta_{m'm}\delta_{j_z'^e j_z^e}\delta_{j_z'^h j_z^h}. \qquad (7)$$

With the aid of (7) and of the ortho-normalization and completeness conditions of functions f_{nlm} we may reverse (5) into ($\alpha = 1 - \beta$)

$$e^+_{q\Gamma j^e j_z^e} h^+_{p\Gamma j^h j_z^h} = V^{-1/2} \sum_{\substack{nlm \\ j^{eh}j^a j_z^a}} S^l_{mj_z^e j_z^h}(j^{eh}, j^a, j_z^a) f^*_{nlm}(\alpha p - \beta q) a^+_{p+q,\, nlj^{eh}j^a j_z^a}. \qquad (8)$$

Note that equation (8) is generalized compared with equation (10) in [19] and equation (7) in [20], where spins were completely ignored.

    Now, before proceeding further, some comments on excitation levels are in order. If the excitation level is high or very high, excitons should not be stable. They must undergo the Mott transition [31], yielding an electron–hole plasma, description of which requires detailed corrections for self-energy, (dynamical) screening and band filling. At medium levels of excitation below the Mott transition, excitons may not be destroyed but must deviate from ideal bosons. Under this circumstance, non-bosonic approaches to the many-exciton system are necessitated (see, e.g., an approach in [19]). In the low excitation limit the non-bosonic behaviour of excitons is small, and up to order $\rho^2 r^6$ (ρ the exciton density) they can be treated as bosons [12] provided that their mutual interaction in a hypothetical bosonic subspace can be adequately formulated to take full account of the fermionic nature of the constitutive quasiparticles of excitons. In what follows we confine ourselves to the low exciton limit and imitate the rigorous, but simple, electron–hole pairing procedure performed in [12] to cast the original fermionic Hamiltonian H^{eh} into the bosonic one H^{a-a} whose part H^{a-a}_{int} describing the interaction among excitons can be written as

$$H^{a-a}_{int} = \tfrac{1}{2} \sum_{pp'q} \sum_{122'1'} U_{122'1'}(p, p', q) a^+_{p+q,1} a^+_{p'-q,2} a_{p',2'} a_{p,1'} \qquad (9)$$

where the abbreviated notations 1, 2, 2' and 1' mean

$$1 = (n_1 l_1 j_1^{eh} j_1^a j_{1z}^a) \qquad 1' = (n_1' l_1' j_1'^{eh} j_1'^a j_{1z}'^a) \qquad \cdots \qquad (10)$$

In equation (9), $U_{122'1'}(p, p', q)$ is determined by

$$U_{122'1'}(p, p', q) = \sum_{m_1 m_2 m_2' m_1'} [U^d_{N_1 N_2 N_2' N_1'}(p, p', q) S^d_{L_1 L_2 L_2' L_1'}(J_1 J_2 J_2' J_1')$$

$$+ U^{ex}_{N_1 N_2 N_2' N_1'}(p, p', q) S^{ex}_{L_1 L_2 L_2' L_1'}(J_1 J_2 J_2' J_1')] \qquad (11)$$

where the abbreviations are $N_1 = (n_1 l_1 m_1)$, $N_1' = (n_1' l_1' m_1'), \ldots;$ $L_1 = (l_1 m_1)$, $L_1' = (l_1' m_1')$; $J_1 = (j_1^{eh} j_1^a j_{1z}^a)$, $J_1' = (j_1'^{eh} j_1'^a j_{1z}'^a), \ldots$. Functions U^d and U^{ex} in (11) are independent of spins and respectively represent 'direct' and 'exchange' inter-excitonic interaction mechanisms. Following [20] we write them down as

$$U^d_{N_1 N_2 N_2' N_1'}(p, p', q) = \sum_{i=1}^{3} U^{(i)}_{N_1 N_2 N_2' N_1'}(p, p', q) \tag{12}$$

$$U^{ex}_{N_1 N_2 N_2' N_1}(p, p', q) = \sum_{i=4}^{6} U^{(i)}_{N_1 N_2 N_2' N_1'}(p, p', q). \tag{13}$$

It can be checked from the general formulae given in [20] for $U^{(i)}$ that for $i = 1, 2, 3$ they depend only on q whereas for $i = 4, 5, 6$ they depend also on $p - p'$ (but not on p and p' separately). Therefore, denoting the difference $p - p'$ by Q we get

$$U^{(1)}_{N_1 N_2 N_2' N_1'}(q) = \frac{F_q}{V} \sum_{k_1} f_{N_1}(k_1 - \beta q) f_{N_1'}^*(k_1) \frac{1}{V} \sum_{k_2} f_{N_2}(k_2 + \beta q) f_{N_2'}^*(k_2) \tag{14}$$

$$U^{(2)}_{N_1 N_2 N_2' N_1'}(q) = \frac{F_q}{V} \sum_{k_1} f_{N_1}(k_1 + \alpha q) f_{N_1'}^*(k_1) \frac{1}{V} \sum_{k_2} f_{N_2}(k_2 - \alpha q) f_{N_2'}^*(k_2) \tag{15}$$

$$U^{(3)}_{N_1 N_2 N_2' N_1'}(q) = -2\frac{F_q}{V} \sum_{k_1} f_{N_1}(k_1 - \beta q) f_{N_1'}^*(k_1) \frac{1}{V} \sum_{k_2} f_{N_2}(k_2 - \alpha q) f_{N_2'}^*(k_2) \tag{16}$$

$$U^{(4)}_{N_1 N_2 N_2' N_1'}(Q, q) = -\frac{1}{V^2} \sum_{k_1} \sum_{k_2} [F_{k_1} f_{N_1}(k_2 - k_1 + \alpha q)$$
$$\times f_{N_2}(k_2 + \beta Q + \beta q) f_{N_2'}^*(k_2 - k_1 + \beta Q + q) f_{N_1'}^*(k_2)] \tag{17}$$

$$U^{(5)}_{N_1 N_2 N_2' N_1'}(Q, q) = -\frac{1}{V^2} \sum_{k_1} \sum_{k_2} [F_{k_1} f_{N_1}(k_2 - k_1 - \beta q)$$
$$\times f_{N_2}(k_2 - \alpha Q - \alpha q) f_{N_2'}^*(k_2 - k_1 - \alpha Q + q) f_{N_1'}^*(k_2)] \tag{18}$$

$$U^{(6)}_{N_1 N_2 N_2' N_1'}(Q, q) = \frac{2}{V^2} \sum_{k_1} \sum_{k_2} [F_{k_1} f_{N_1}(k_2 - k_1 - \beta q)$$
$$\times f_{N_2}(k_2 - \alpha Q - \alpha q) f_{N_2'}^*(k_2 - \alpha Q - q) f_{N_1'}^*(k_2)]. \tag{19}$$

Effects caused by spins are governed by the spin-dependent symbols S^d and S^{ex}, which are sums of products of Clebsch–Gordan coefficients. Namely, they are of the forms

$$S^d_{L_1 L_2 L_2' L_1'}(J_1 J_2 J_2' J_1') = \sum_{j_{1z}^e} \sum_{j_{1z}^h} \sum_{j_{2z}^e} \sum_{j_{2z}^h} S^{l_1}_{m_1 j_{1z}^e j_{1z}^h}(J_1) S^{l_2}_{m_2 j_{2z}^e j_{2z}^h}(J_2) S^{l_2'}_{\bar{m}_2 j_{2z}^e j_{2z}^h}(J_2') S^{l_1'}_{\bar{m}_1 j_{1z}^e j_{1z}^h}(J_1')$$
$$\tag{20}$$

$$S^{ex}_{L_1 L_2 L_2' L_1'}(J_1 J_2 J_2' J_1') = \sum_{j_{1z}^e} \sum_{j_{1z}^h} \sum_{j_{2z}^e} \sum_{j_{2z}^h} S^{l_1}_{m_1 j_{1z}^e j_{1z}^h}(J_1) S^{l_2}_{m_2 j_{2z}^e j_{2z}^h}(J_2) S^{l_2'}_{\bar{m}_2 j_{2z}^e j_{2z}^h}(J_2') S^{l_1'}_{\bar{m}_1 j_{2z}^e j_{1z}^h}(J_1').$$
$$\tag{21}$$

For the simplest but most significant case when all of the excitons are in the ground state and $j^e = j^h = 1/2$ (as for the yellow excitonic series of Cu_2O) we have $j^{eh} = j^a$,

$$S^d(J_1 J_2 J_2' J_1') = \delta_{J_1' J_1} \delta_{J_2' J_2} \tag{22}$$

and

$$S^{ex}(J_1 J_2 J_2' J_1') = S^{ex}(J_2 J_1 J_1' J_2') = S^{ex}(J_1' J_2' J_2 J_1) = S^{ex}(J_2' J_1' J_1 J_2). \tag{23}$$

Then equation (9) looks quite simple:

$$H_{int}^{a-a} = \frac{1}{2}\left(\sum_q U^d(q) \sum_{pp'} \sum_{J_1 J_2} a_{p+q,J_1}^+ a_{p'-q,J_2}^+ a_{p',J_2} a_{p,J_1} + \sum_{pp'q} U^{ex}(p - p' = Q, q)\right.$$

$$\left. \times \sum_{J_1 J_2 J_2' J_1'} S^{ex}(J_1 J_2 J_2' J_1') a_{p+q,J_1}^+ a_{p'-q,J_2}^+ a_{p',J_2'} a_{p,J_1'}\right). \tag{24}$$

In (22)–(24) and from now on for brevity we drop all the indices N_i and L_i in $U^{d(ex)}$ and $S^{d(ex)}$ understanding that they are '100' and '00' for excitons in the ground state, respectively.

At this point it can be noted that though many-exciton Hamiltonians have been found by many authors [5, 7–9, 11–13, 20] using different methods of derivation, those given here by equations (9) and (24) take into account explicitly for the first time the spin of the quasiparticles. In the next section we shall show that for small momenta the character of the exciton–exciton interaction is essentially determined by the symmetry of the spin function of two interacting excitons, but for larger momenta the q, Q and s dependences will give important influences.

3. Spin-dependent exciton–exciton interaction potential

In this section we shall derive analytical expressions for the exciton–exciton interaction potential, which is anticipated to be less than the exciton binding energy. That means that interactions between excitons do not destroy them to generate free electron–hole pairs. For the S-type excitons and with the spin–orbit coupling neglected, excitons may belong to two kinds: the para- ($j^a = j_z^a = 0$) and the ortho-exciton ($j^a = 1$; $j_z^a = 0, \pm 1$). Denote by $|k_1 k_2 j^a j^b j j_z\rangle$ the zero-order approximation state vector of two excitons, one of which possesses momentum k_1 (k_2), spin j^a (j^b) and the other has momentum k_2 (k_1), spin j^b (j^a) and whose total spin and its projection equal j and j_z. Owing to group-theoretical methods, the table for the values of Clebsch–Gordan coefficients and the symmetry requirements for a two-boson system, we can construct the spin-symmetric possible two-exciton state vectors $|k_1 k_2\ 00\ 00\rangle$, $|k_1 k_2\ 10\ 1m\rangle$ ($m = 0, \pm 1$), $|k_1 k_2\ 11\ 2m\rangle$ ($m = 0, \pm 1, \pm 2$), $|k_1 k_2\ 11\ 1m\rangle$ ($m = 0, \pm 1$) and $|k_1 k_2\ 11\ 00\rangle$. For a given value of m, say, $m = 1$, we have

$$|k_1 k_2\ 00\ 00\rangle = a_{k_100}^+ a_{k_200}^+ |0\rangle \tag{25}$$

$$|k_1 k_2\ 10\ 11\rangle = (1/\sqrt{2})(a_{k_111}^+ a_{k_200}^+ + a_{k_100}^+ a_{k_211}^+)|0\rangle \tag{26}$$

$$|k_1 k_2\ 11\ 21\rangle = (1/\sqrt{2})(a_{k_111}^+ a_{k_210}^+ + a_{k_110}^+ a_{k_211}^+)|0\rangle \tag{27}$$

$$|k_1 k_2\ 11\ 11\rangle = (1/\sqrt{2})(a_{k_111}^+ a_{k_210}^+ - a_{k_110}^+ a_{k_211}^+)|0\rangle \tag{28}$$

$$|k_1 k_2 \, 11 \, 00\rangle = (1/\sqrt{3})(a^+_{k_1 11} a^+_{k_2 1-1} - a^+_{k_1 10} a^+_{k_2 10} + a^+_{k_1 1-1} a^+_{k_2 11})|0\rangle. \qquad (29)$$

'Sandwiching' Hamiltonian (22) between two-exciton state vectors and accounting for the definition (21), which gives

$$S^{\text{ex}}(J_1 J_2 J'_2 J'_1) = \begin{cases} 1 & \text{if } J_1 = J_2 = J'_2 = J'_1 = 11, 1-1 \\ & \begin{cases} \{J_1, J_2\} = \{J'_1, J'_2\} = \{00, 00\}, \{10, 00\} \\ \frac{1}{2} & \text{if } \{J_1, J_2\}(\{J'_1, J'_2\}) = \{10, 10\} \text{ while} \\ & \{J'_1, J'_2\} = \{J_1, J_2\} = \{11, 1-1\} \end{cases} \\ 0 & \text{otherwise} \end{cases} \qquad (30)$$

(symbol equalities $\{J_1, J_2\} = \{ab, cd\}$ mean either $J_1 = ab, J_2 = cd$ or $J_1 = cd, J_2 = ab$), we are able to calculate the various necessary matrix elements that would offer corresponding dependences on Q, q and s of the interaction between:

(i) two para-excitons

$$W_{\pi-\pi}(\ldots) = \langle p + q, p' - q \, 00 \, 00|H^{a-a}_{\text{int}}|pp' \, 00 \, 00\rangle = U^d(q) + U^d(Q + q)$$
$$+ \tfrac{1}{2}[U^{\text{ex}}(Q, q) + U^{\text{ex}}(Q, -Q - q)] \qquad (31)$$

(ii) an ortho- and a para-exciton

$$W_{0-\pi}(\ldots) = \tfrac{1}{3} \sum_{m=0,\pm 1} \langle p + q, p' - q \, 10 \, 1m|H^{a-a}_{\text{int}}|pp' \, 10 \, 1m\rangle = U^d(q) + U^d(Q + q)$$
$$+ U^{\text{ex}}(Q, q) + U^{\text{ex}}(Q, -Q - q) \qquad (32)$$

(iii) two ortho-excitons with $j = 2$

$$W_{0-0, j=2}(\ldots) = \tfrac{1}{5} \sum_{m=0,\pm 1, \pm 2} \langle p + q, p' - q \, 11 \, 2m|H^{a-a}_{\text{int}}|pp' \, 11 \, 2m\rangle \equiv W_{0-\pi}(\ldots) \qquad (33)$$

(iv) two ortho-excitons with $j = 1$

$$W_{0-0, j=1}(\ldots) = \tfrac{1}{3} \sum_{m=0,\pm 1} \langle p + q, p' - q \, 11 \, 1m|H^{a-a}_{\text{int}}|pp' \, 11 \, 1m\rangle = U^d(q) - U^d(Q + q) \qquad (34)$$

(v) and two ortho-excitons with $j = 0$

$$W_{0-0, j=0}(\ldots) = \langle p + q, p' - q \, 11 \, 00|H^{a-a}_{\text{int}}|pp' \, 11 \, 00\rangle = U^d(q) + U^d(Q + q)$$
$$- \tfrac{1}{2}[U^{\text{ex}}(Q, q) + U^{\text{ex}}(Q, -Q - q)] \qquad (35)$$

where $(\ldots) \equiv (p - p' = Q, q)$.

Analytical differences in equations (31) to (35) clearly stress the role that the spin symmetry of the two-exciton state vectors plays in connection with the character of exciton–exciton mutual interaction. To see things quantitatively, we have to evaluate

the expressions (31)–(35). Such a task might be done analytically just in a proper approximation, which will be presented in the forthcoming section.

4. Approximation for analytical calculation

Mathematically exciton–exciton interaction potentials (31)–(35) depend on U^d and U^{ex} in (12) and (13), which are in turn determined by $U^{(i)}$ ($i = 1$–6) in (14)–(19). Therefore, knowing the way to calculate $U^{(i)}$ is necessary. However, being complicated functionals of f_{nlm}, in principle $U^{(i)}$ cannot be analytically calculated for arbitrary momenta and electron–hole mass ratio [8]. Even in the case of S-type exciton wavefunctions and a certain value of s, numerical evaluations of $U^{(i)}$ take a very long computer time because of the iteration process that is needed to resolve the seeming logarithmic divergence in order to get results with a desired accuracy [10]. For that reason, many authors have evaluated the potentials only in limiting cases, namely $Q = q = 0$ [2–8, 21, 24–26] (in this case the s dependence disappears [20]) or $Q = 0$, $q \neq 0$, $s = 0$ [8], 1/8 and 1 [4]. To calculate $U^{(i)}$ analytically throughout the whole range of Q, q and s one has to resort to an appropriate approximation. In [29] an approximation was suggested, which replaced fractional functions by exponent ones. This replacement results in more rapid decreasing of exciton wavefunctions with increasing momentum in the large momentum region. It leads, for example, to some modification of the far tails of the exciton luminescence zone but does not significantly change qualitative behaviours. The criterion of validity of the approximation is $k_0 T / I_{2D(3D)} \ll \alpha\beta$, where k_0 and T are the Boltzmann constant and temperature (see [29]). Such an approximation works very well in the small momentum limit. Yet, regarding the behaviours of the approximated exciton wavefunctions in the whole range of momentum, they do not satisfy the physically meaningful normalization condition. Here, as in [20], we improve this shortcoming by multiplying the approximated (exponent) exciton wavefunctions by constants C_{nlm} that again guarantee that the functions become normalized. C_{nlm} prove to be distinctive for different exciton relative motion states, i.e. for different nlm. For the 1S-type functions, we have $C_{1S}^{2D} = (3/2)^{1/2}$ and $C_{1S}^{3D} = \pi^{1/4}$. Consequently, the corresponding 2D and 3D exciton wavefunctions in the ground state read

$$f^{2D}(p) = \frac{2(2\pi)^{1/2} r_{2D}}{(1 + r_{2D}^2 p^2)^{3/2}} \simeq 2(3\pi)^{1/2} r_{2D} \exp(-3r_{2D}^2 p^2/2) \tag{36}$$

$$f^{3D}(p) = \frac{8(\pi r_{3D}^3)^{1/2}}{(1 + r_{3D}^2 p^2)^2} \simeq 8\pi^{3/4} r_{3D}^{3/2} \exp(-2r_{3D}^2 p^2). \tag{37}$$

The advantage of the approximations (36) and (37) rests in the fact that they enable us to integrate (14)–(19) analytically, avoiding long computer time numerical multifold integrations. Putting (36) and (37) together with the 2D and 3D Coulomb forces $F_q^{2D} = 2\pi e^2/\varepsilon q V_{2D}$ and $F_q^{3D} = 4\pi e^2/\varepsilon q^2 V_{3D}$ (e and ε are the electron charge and the static dielectric constant) into (14)–(19) and then replacing in them sums by integrals, we have performed the analytical integrations for $U^{(i)}$ [20]. Substituting them into (12) and (13) gives U^d and U^{ex} in forms that look quite easy to handle for further theoretical calculations:

$$U_{2D}^d(q) = (2\pi G_{2D}/q r_{2D})[\exp(-3\alpha^2 q^2 r_{2D}^2/4) - \exp(-3\beta^2 q^2 r_{2D}^2/4)]^2 \tag{38}$$

$$U_{3D}^d(q) = (8\pi G_{3D}/q^2 r_{3D}^2)[\exp(-\alpha^2 q^2 r_{3D}^2) - \exp(-\beta^2 q^2 r_{3D}^2)]^2 \tag{39}$$

$$U_{2D}^{ex}(Q, q) = \frac{(3\pi/2)^{1/2}G_{2D}}{3}\left(4\sqrt{3}\exp\{-\tfrac{3}{2}r_{2D}^2[\alpha^2(Q + q)^2 + \beta^2 q^2]\}\right.$$

$$\times \int_0^{2\pi} \exp\{r_{2D}^2[\alpha(Q + q) - \beta q]^2 \cos^2(x/2)\}\,dx$$

$$- 3\exp\{-\tfrac{3}{2}r_{2D}^2[\alpha^2(Q + q)^2 + \beta^2 q^2]\}\int_0^{2\pi}\exp[3r_{2D}^2\beta^2 q^2 \cos^2(x/2)]\,dx$$

$$- 3\exp\{-\tfrac{3}{2}r_{2D}^2[\beta^2(Q + q)^2 + \alpha^2 q^2]\}$$

$$\left.\times \int_0^{2\pi} \exp[3r_{2D}^2\alpha^2 q^2 \cos^2(x/2)]\,dx\right) \tag{40}$$

$$U_{3D}^{ex}(Q, q) = \frac{32\pi G_{3D}}{3}\left(4\sqrt{3}\exp\{-2r_{3D}^2[\alpha^2(Q + q)^2 + \beta^2 q^2]\}\right.$$

$$\times \int_0^1 \exp\{\tfrac{8}{3}r_{3D}^2[\alpha(Q + q) - \beta q]^2 x^2\}\,dx$$

$$- 3\exp\{-2r_{3D}^2[\alpha^2(Q + q)^2 + \beta^2 q^2]\}\int_0^1\exp(2r_{3D}^2\beta^2 q^2 x^2)\,dx$$

$$\left.- 3\exp\{-2r_{3D}^2[\beta^2(Q + q)^2 + \alpha^2 q^2]\}\int_0^1\exp(2r_{3D}^2\alpha^2 q^2 x^2)\,dx\right) \tag{41}$$

where

$$G_{2D}\ (G_{3D}) = I_{2D}r_{2D}^2 V_{2D}^{-1}(I_{3D}r_{3D}^3 V_{3D}^{-1}).$$

5. Graphical demonstration

As follows straightforwardly from (31)–(35) and from (38)–(41), the Q, q and s (i.e. α, β) dependences of the exciton–exciton interaction potentials are analytically explicit. This allows us easily to program a computer to plot the variation of the potentials throughout the whole range of Q, q and s. Relative contributions from different physically possible mechanisms $U^{(i)}$ ($i = 1$–6) to the spin-independent exciton–exciton interaction were clear in [20] (see, e.g., figures 2, 3, 5 and 6 therein) in respect of the q and s dependences in both 2D and 3D cases. The spinless quasiparticle treatment in [20] is in a sense equivalent to that of a para-exciton gas in which excitons with equal momenta always repel one other if their momentum transfer is zero. We shall show that with quasiparticle spins being taken into consideration the character of the exciton–exciton interaction might be either repulsive or attractive depending delicately not only on the spin symmetry of two-exciton states but also on all of the variables entering formulae (31)–(35). For convenience in presenting figure axis titles we introduce the following normalized dimensionless notations: $W2D(\text{pa–pa}) \equiv G_{2D}^{-1}W_{\pi-\pi}^{2D}$; $W2D(\text{or–pa}) \equiv G_{2D}^{-1}W_{o-\pi}^{2D}$; $W2D(\text{or–or}, 2) \equiv G_{2D}^{-1}W_{o-o,2}^{2D}$; $W2D(\text{or–or}, 1) \equiv G_{2D}^{-1}W_{o-o,1}^{2D}$; $W2D(\text{or–or}, 0) \equiv G_{2D}^{-1}W_{o-o,0}^{2D}$; $W3D(\text{pa–pa}) \equiv G_{3D}^{-1}W_{\pi-\pi}^{3D}$; $\ldots$; $qr[2D] \equiv qr_{2D}$; $Qr[2D] \equiv Qr_{2D}$; $\ldots$.

We have plotted many figures, some of which will be shown below. Figure 1 represents 2D normalized interaction potentials between two para-excitons with equal
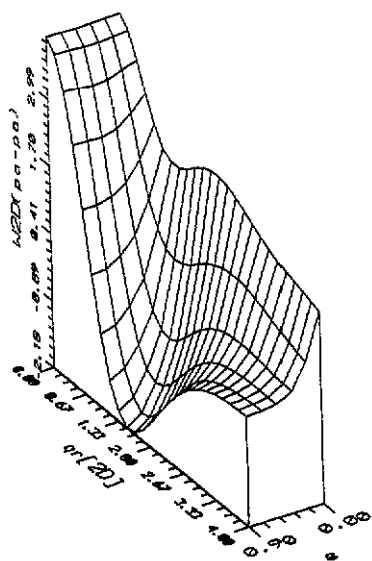
Figure 1. 2D normalized interaction potentials between two para-excitons with equal momenta versus electron–hole mass ratio s and momentum transfer qr_{2D}.
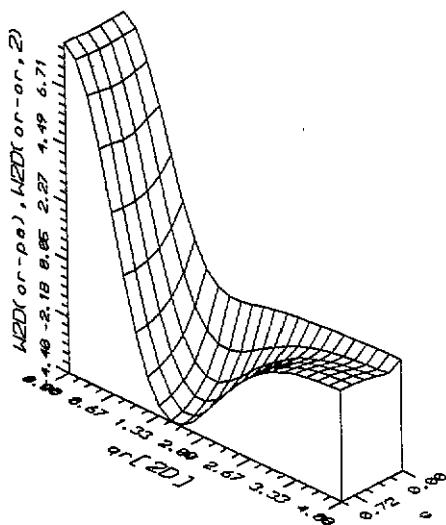

Figure 2. The same as in figure 1 but between an ortho-exciton and a para-exciton (or between two ortho-excitons with total spin $j = 2$).
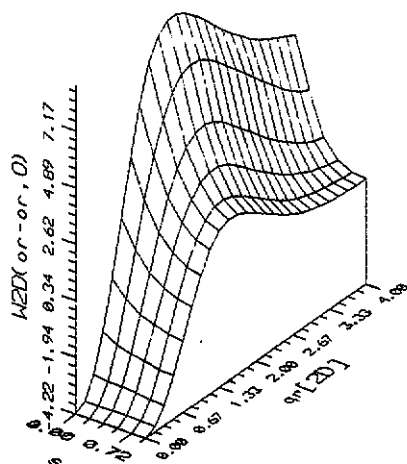

Figure 3. The same as in figure 1 but between two ortho-excitons with total spin $j = 0$.

momenta as functions of s and of qr_{2D}. At $qr_{2D} = 0$ all the potentials take an equal positive value independent of s. For small decrease in qr_{2D} potential magnitudes decrease quite rapidly but still remain positive. When qr_{2D} is increasing further, the potentials begin to behave differently in accordance with s. By direct inspection of figure 1 one sees that for $s = 0.9$ (0.72 or 0.54) the potential vanishes at $qr_{2D} \simeq 0.84$ and then becomes more and more negative, reaching a minimum at $qr_{2D} \simeq 1.66$ (1.55 or 1.50). After that it increases again and, conserving the sign, tends to zero for $qr_{2D} \to \infty$ (in fact for qr_{2D}
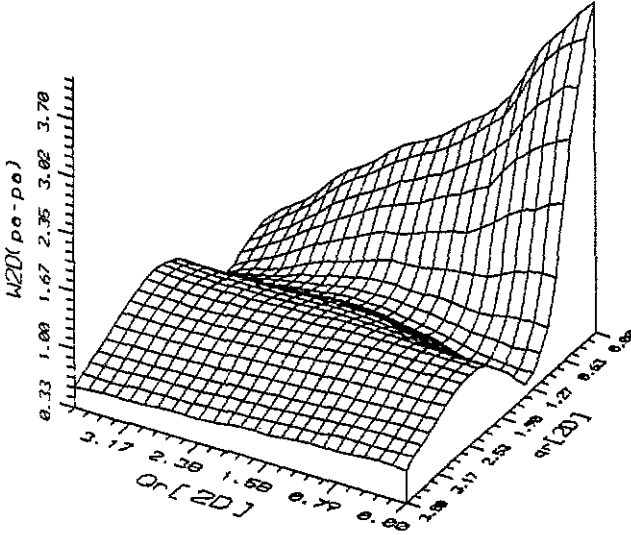
Figure 4. 2D normalized interaction potentials between two para-excitons versus exciton momentum difference Qr_{2D} and momentum transfer qr_{2D}. The case of $s = 0.2$ and of geometrical configuration $Q \perp q$.

larger than 4). For $s = 0.36$ there appears an interval of qr_{2D} ranging from 0.85 to 2.00 inside (outside) of which the interaction is attractive (repulsive). The potential signs in the case of $s = 0.18$ and 0 are, however, always positive in the whole domain of qr_{2D}. The comments made clearly indicate the role not only of spin combination symmetry but also of momentum transfer and electron–hole mass ratio in determining the exciton–exciton interaction character. Similar comments hold for interaction potentials between an ortho-exciton and a para-exciton and between two ortho-excitons with total spin $j = 2$ (see figure 2). In figure 3 the opposite situation happens when two ortho-excitons with equal momenta and total spin $j = 0$ attract each other for small qr_{2D} and arbitrary s. With a given relatively small value of s, attraction might turn into repulsion if qr_{2D} increases properly. For relatively large s (see, e.g., curves with $s = 0.72$ and 0.90 in figure 3) $W^{2D}_{o-o, j=0}$ are negative for any qr_{2D}. Crudely speaking, figures 1 and 3 look upside down. As to $W^{2D}_{o-o, j=1}$ it identically vanishes for any q and s if $Q = 0$ (see (34)).

The q and Q dependences of $W^{2D(3D)}$ can be plotted for s and the angle between vectors q and Q fixed as parameters. They are represented in figures 4 to 7 respectively for $W^{2D}_{\pi-\pi}$, $W^{2D}_{o-\pi}$ ($W^{2D}_{o-o, j=2}$), $W^{2D}_{o-o, j=1}$ and $W^{2D}_{o-o, j=0}$ for $s = 0.2$ and $q \perp Q$. As it must be, one can observe from figure 7 that $W^{2D}_{o-o, 1}(0, q) \equiv 0$.

As for the 3D figures (not shown) they look, for the reason explained in [20, 24], qualitatively quite similar to the corresponding 2D ones, except for the fact that the exciton–exciton interaction potentials in the 3D case are remarkably enhanced as compared with those in the 2D one. The binding energy of a 2D exciton is, on the contrary, four times larger than that of a 3D one.

6. Conclusion and discussion

Summing up the results we have approximately derived analytical expressions of the exciton–exciton interaction potentials in both 2D and 3D materials, which depend
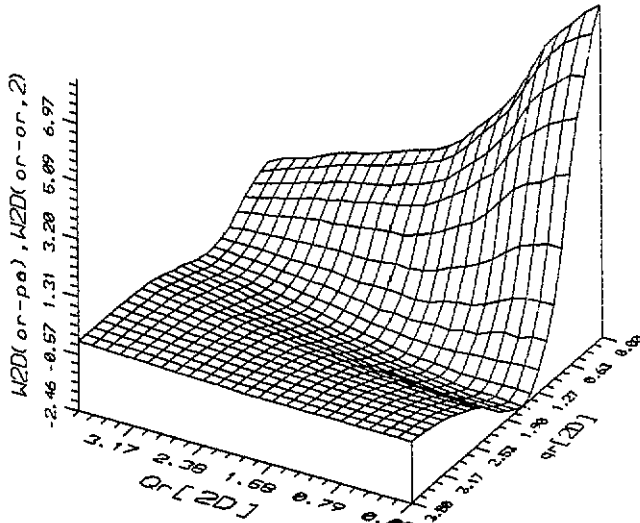
Figure 5. The same as in figure 4 but between an ortho-exciton and a para-exciton (or between two ortho-excitons with total spin $j = 2$).
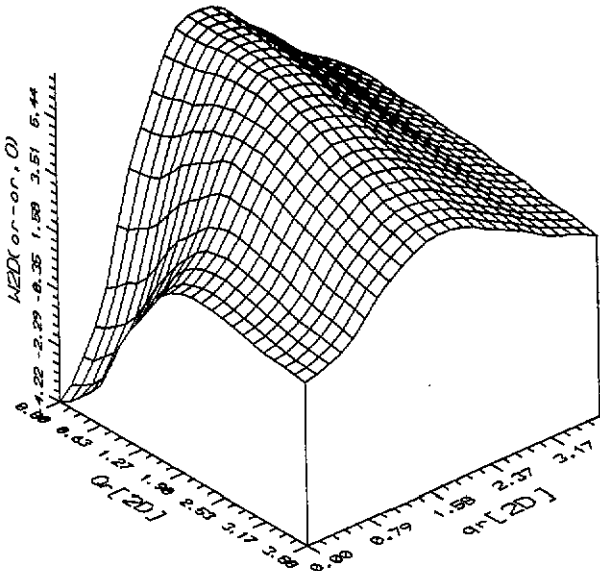

Figure 6. The same as in figure 4 but between two ortho-excitons with total spin $j = 0$.

explicitly on exciton momentum difference, momentum transfer, electron–hole mass ratio and two-exciton state spin symmetry. Our results hold on the basis of the concept of para- and ortho-excitons, which is valid when the para–ortho exciton splitting is greater than the exciton–exciton interaction energy. Such a condition is met, for example, in RbBr, KBr, NaBr or for the yellow excitonic series in Cu_2O. While the 3D
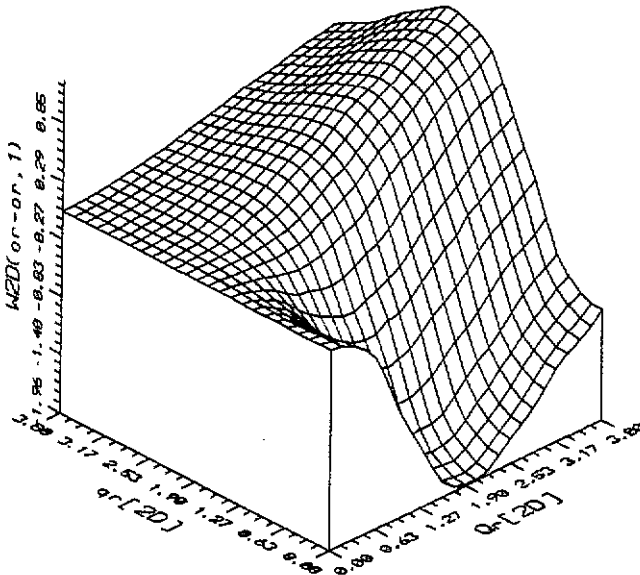
Figure 7. The same as in figure 4 but between two ortho-excitons with total spin $j = 1$.

results suit 'bulk' media, the 2D ones could be applicable to 'planar' excitons at, for example, the Tamm surface or at the boundary between a crystal and vacuum. In the latter situation the static dielectric constant ε screening the Coulomb force should be replaced by $(\varepsilon + 1)/2$ [32]. The 2D results could also be generalized for a more realistic quasi-2D structure, a quantum well one, which, of course, must include many other effects such as well and barrier width dependences, finite barrier height, in-plane correlation of electrons and holes, hole mass anisotropy, image charges, etc. The role that the exciton–exciton interaction plays in causing bistability [14, 16] and anomalies of polariton dispersion curves [15, 18] was considered. In [17], we used a non-bosonic approach to propose a possible method for determining the effective exciton–exciton interaction constant by measuring dispersion curves of the lower polariton energy branches under different levels of excitation. Nevertheless, account of spin was still omitted in all papers quoted above. We hope that taking into account the quasiparticle spin might bring about new results to those in [15–19], as this paper does with respect to [20].

Acknowledgments

References

[1] Culik F 1966 *Czech. J. Phys.* **16** 194

[2] Keldysh L V and Kozlov A N 1968 *Sov. Phys.–JETP* **54** 978
[3] Hanamura E 1970 *J. Phys. Soc. Japan* **29** 50
[4] Bobrysheva A I, Miglei M F and Smiglyuk M I 1972 *Phys. Status Solidi* b **53** 71
[5] Hanamura E 1974 *J. Phys. Soc. Japan* **37** 1545
[6] Bobrysheva A I, Moskalenko S A and Vybornov V I 1976 *Phys. Status Solidi* b **76** K51
[7] Haug H 1976 *Z. Phys.* B **24** 351
[8] Hanamura E and Haug H 1977 *Phys. Rep.* **33** 209
[9] Stoltz H, Zimmermann R and Ropke G 1981 *Phys. Status Solidi* b **105** 585
[10] Nguyen Ba An, Nguyen Van Hieu *et al* 1981 *Ann. Phys.* **31** 149
[11] Steyn-Ross M L and Gardiner C W 1983 *Phys. Rev.* A **27** 310
[12] Haug H and Schmitt-Rink S 1984 *Prog. Quantum Electron.* **9** 3
[13] May V, Boldt F and Henneberger K 1985 *Phys. Status Solidi* b **129** 717
[14] Nguyen Ba An 1988 *Phys. Status Solidi* b **150** 845
[15] Nguyen Ba An 1989 *J. Phys.: Condens. Matter* **1** 9843
[16] Nguyen Ba An 1990 *J. Physique* **51** 1
[17] Nguyen Ba An 1990 *Phys. Scr.* **42** 741
[18] Nguyen Ba An and Hoang Xuan Nguyen 1990 *Phys. Lett.* A **144** 45
[19] Nguyen Ba An and Hoang Ngoc Cam 1990 *J. Phys.: Condens. Matter* **2** 4127
[20] Nguyen Ba An and Hoang Ngoc Cam 1991 *Czech. J. Phys.* B **41**
[21] Bobrysheva A I, Zyukov V Y and Beryl S I 1980 *Phys. Status Solidi* **101** 69
[22] Peyghambarian N *et al* 1984 *Phys. Rev. Lett.* **53** 2433
[23] Chemla D S and Miller D A B 1985 *J. Opt. Soc. Am.* B **2** 1155
[24] Manzk G, Henneberger K and May V 1987 *Phys. Status Solildi* b **139** 233
[25] Hiroshima T, Hanamura E and Yamanishi M 1988 *Phys. Rev.* B **38** 1241
[26] Hiroshima T 1989 *Phys. Rev.* B **40** 3862
[27] Schmitt-Rink S, Chemla D S and Miller D A B 1989 *Adv. Phys.* **38** 89
[28] Boldt F, Henneberger K and May V 1985 *Phys. Status Solildi* b **130** 675
[29] Khadzi P I 1977 *Kinetika Recombinaxionnovo Izluchenija Eksitonov i Bieksitonov v Poluprovodnikakh* (Kishinev: Shtiintxa)
[30] Edmonds A R 1957 *Angular Momentum in Quantum Mechanics* (Princeton, NJ: Princeton University Press)
[31] Zimmermann R 1988 *Phys. Status Solidi* b **146** 371
[32] Ginzburg V L and Kelle V V 1973 *Pis. Zh. Eksp. Teor. Fiz.* **17** 428